SPATIAL FILTERING OF NEAR-FIELD RADIO FREQUENCY INTERFERENCE AT A LOFAR LBA STATION

Jan-Willem W. Steeb, David B. Davidson *

Department of Electrical and Electronic Engineering
Stellenbosch University
Stellenbosch, South Africa
davidson@sun.ac.za

Stefan J. Wijnholds

R&D Department
ASTRON
Dwingeloo, The Netherlands
wijnholds@astron.nl
and Dept E&E Eng,
Stellenbosch University

ABSTRACT

In preparation for the SKA, many new RFI (radio frequency interference) mitigation algorithms have been developed. However, these algorithms usually assume that the RFI source is in the far-field and that the array is calibrated. In this paper, the recovery of astronomical signals from uncalibrated RFI-corrupted LOFAR visibility data using spatial filtering methods are presented. For this demonstration, a near-field continuous-wave RFI source was generated by a hexacopter that was flown around one of the LOFAR LBA (low-band antenna) arrays. Four spatial filtering methods were applied to the RFI contaminated data: orthogonal projection, orthogonal projection with subspace bias correction, oblique projection and subspace subtraction. Overall, orthogonal projection with subspace bias correction performed the best, however it requires that the RFI source moves relative to the array and it is computationally expensive. Oblique projection performs similar to orthogonal projection with subspace bias correction when point sources are to be recovered and is furthermore considerably less computationally expensive. Subspace subtraction is a suitable alternative if a large field of view is to be recovered at a relatively low computational cost.

Index Terms— RFI mitigation, LOFAR, near-field RFI, spatial filtering.

1. INTRODUCTION

LOFAR is part of a new generation of radio telescope arrays with large bandwidths, high sensitivity and resolution. To obtain high resolutions long baselines are required and therefore most RFI sources will be in the near-field. Consequently, powerful near-field RFI presents a serious challenge. In this paper the application of spatial RFI mitigation techniques to uncalibrated data which has been corrupted with a near-field source is presented. The experimental setup is explained, followed by a description of the mathematical model and applied RFI mitigation techniques. Finally, the experimental results are given.

2. EXPERIMENTAL SETUP

For this demonstration, a near-field continuous-wave RFI source was generated by a hexacopter that was flown around the LOFAR LBA (low-band antenna) array CS302. A signifcant feature of this test is that the hexacopter's flight path was within the array's near-field. The Rayleigh distance for a LOFAR station is approximately 1900 m for a given longest baseline of approximately 85 m and a wavelength of 6.74 m (the sub-band with centre frequency 44.5095 MHz was used).

3. MODEL

The following general model (used in [1, 2, 3, 4, 5]) is considered for the output generated at time t by an antenna array that consists of N_e elements, for one polarization and frequency channel:

$$\mathbf{y}(t) = \mathbf{g} \odot (\mathbf{x}_c(t) + \mathbf{x}_r(t)) + \mathbf{x}_n(t) \quad (1)$$

*This work is supported by SKA South Africa, the South African Research Chairs Initiative of the Department of Science and Technology, the National Research Foundation, and a Marie Curie International Research Staff Exchange Scheme Fellowship within the 7th European Community Framework Programme MIDPREP, Grant Agreement PIRSES-GA-2013-612599.

The authors would like to thank Millad Sardarabadi for the fruitful discussions and useful feedback.

where

$\mathbf{y}(t)$	is an $N_e \times 1$ vector of measured array output signals,
$\mathbf{g}$	is the vector of complex gains for each antenna,
$\odot$	Hadamard product,
$\mathbf{x}_c(t)$	is the vector where each element is the sum of N_c delayed cosmic signals for a given antenna,
$\mathbf{x}_r(t)$	is the vector where each element is the sum of N_r delayed RFI signals for a given antenna,
$\mathbf{x}_n(t)$	is the vector of instrumental noise for each antenna.

The gains $\mathbf{g}$ are unknown, since the array is assumed to be uncalibrated.

The frequency channel is assumed to be sufficiently narrowband, so that the time delays τ can be represented as phase delays. Therefore, a delayed signal can be approximated by $s(t-\tau) \approx s(t)e^{-i2\pi\nu_0\tau}$, where ν_0 is the centre frequency of the channel. This condition is satisfied for the array, if $2\pi\Delta\nu\tau_{max} \ll 1$, where $\Delta\nu$ is the signal's bandwidth and τ_{max} is the delay given by the longest baseline (greatest distance between any two antennas) [6].

The phase delays for the k^{th} RFI source can be stacked into a vector that is called the geometric delay vector

$$\mathbf{a}_{r_k} = \begin{bmatrix} e^{-i2\pi\nu_0\tau_{1r_k}} \\ \vdots \\ e^{-i2\pi\nu_0\tau_{N_e r_k}} \end{bmatrix}. \tag{2}$$

An $N_e \times N_r$ matrix can now be constructed from the geometric delay vectors, $\mathbf{A}_r = [\mathbf{a}_{r_1} \dots \mathbf{a}_{r_{N_r}}]^T$ (the same applies for the cosmic signals, $\mathbf{A}_c = [\mathbf{a}_{c_1} \dots \mathbf{a}_{c_{N_c}}]^T$), and therefore the model in equation 1 can be written as

$$\mathbf{y}(t) = \mathbf{g} \odot (\mathbf{A}_c\mathbf{s}_c(t) + \mathbf{A}_r\mathbf{s}_r(t)) + \mathbf{x}_n(t), \tag{3}$$

where $\mathbf{s}_c(t)$ and $\mathbf{s}_r(t)$ are respectively, the vectors of the cosmic and RFI signals without delays.

The zero lag covariance matrix (the ij^{th} element of the matrix is the covariance of the i^{th} and j^{th} antenna [7, p. 501]) of the vectorised data model in equation 1 is given by

$$\mathbf{R} = \mathbb{E}\{\mathbf{y}(t)\mathbf{y}^H(t)\}, \tag{4}$$

where $\mathbb{E}$ is the expectation, ^{H} is the Hermitian transpose or complex conjugate transpose and it is assumed that for a given time period none of the signals change position. Therefore, the covariance is constant over this time period as long as the signals are themselves stationary.

Independence between the cosmic, RFI and noise sources is assumed, therefore, when substituting equation 3 into equation 4 the expectation of any non-self multiplication terms is zero and consequently the substitution yields

$$\begin{aligned} \mathbf{R} &= \mathbf{G}(\mathbf{R}_c + \mathbf{R}_r)\mathbf{G}^H + \mathbf{R}_n \\ &= \mathbf{G}(\mathbf{A}_c\mathbf{B}_c\mathbf{A}_c^H + \mathbf{A}_r\mathbf{B}_r\mathbf{A}_r^H)\mathbf{G}^H + \mathbf{R}_n, \end{aligned} \tag{5}$$

where $\mathbf{B}_c = \mathbb{E}\{\mathbf{s}_c(t)\mathbf{s}_c^H(t)\}$, $\mathbf{B}_r = \mathbb{E}\{\mathbf{s}_r(t)\mathbf{s}_r^H(t)\}$, $\mathbf{R}_n = \mathbb{E}\{\mathbf{x}_n(t)\mathbf{x}_n^H(t)\}$ and $\mathbf{G}$ is the diagonal matrix of $\mathbf{g}$. The matrices $\mathbf{B}_c$ will be diagonal if the cosmic signals are uncorrelated and the same applies to $\mathbf{B}_r$ and $\mathbf{R}_n$ if the RFI and noise signals are, respectively, uncorrelated. Since the signals are spatially and temporally stationary, the covariance matrix is estimated by

$$\widehat{\mathbf{R}} = \frac{1}{N_t}\sum_{i=1}^{N_t} \mathbf{y}(iT_s)\mathbf{y}^H(iT_s), \tag{6}$$

where

$\widehat{\mathbf{R}}$	is the estimated covariance matrix,
N_t	is the number of samples for which the signals are stationary,
T_s	is the sample time.

The covariance matrix has the following useful properties: $\mathbf{R}$ is Hermitian and is positive semi-definite [8, p. 558].

4. SPATIAL RFI MITIGATION

4.1. Orthogonal Projection

If the columns of $\mathbf{A}_r$ are linearly independent, they form a basis for a vector space V_r. Therefore, an orthogonal projector can be constructed [8, p. 430] which projects along V_r onto a vector space orthogonal to V_r , namely

$$\mathbf{P} = \mathbf{I} - \mathbf{A}_r(\mathbf{A}_r^H\mathbf{A}_r)^{-1}\mathbf{A}_r^H, \tag{7}$$

such that $\mathbf{PA}_r = \mathbf{0}$. The projector is Hermitian and therefore $\mathbf{P} = \mathbf{P}^H$ [8, p. 433]. Applying the projector to equation 5 yields (assuming $\mathbf{G} = \mathbf{I}$)

$$\begin{aligned} \mathbf{PRP} =& \mathbf{PR}_c\mathbf{P} + \mathbf{PA}_r\mathbf{B}_r\mathbf{A}_r^H\mathbf{P} + \mathbf{PR}_n\mathbf{P} \\ =& \mathbf{PR}_c\mathbf{P} + \mathbf{PR}_n\mathbf{P} \\ =& \mathbf{PR}_{cn}\mathbf{P}. \end{aligned} \tag{8}$$

The RFI contribution to the covariance is completely nulled; however, the noise and cosmic signals are biased.

4.2. Orthogonal Projection with Subspace Bias Correction

For any useful orthogonal projector $\mathbf{P}$ the kernel basis includes the zero vector and at least one non-zero vector, therefore, $\mathbf{P}$ has a column rank less than the number of columns in $\mathbf{P}$ which consequently makes the matrix singular. The orthogonal projection method bias (see equation 8) can therefore not be corrected by multiplying with the inverted orthogonal projector.

For the orthogonal projection correction scheme ([2, 3, 4]) the number of samples N_t is divided into N_G equally sized groups, where each group consists of N_{st} samples (st denotes short term), that is, $N_t = N_G N_{st}$. For a sampling time T_s the overall integration time is $N_t T_s$, while $N_{st}T_s$ is the short term integration time for any of the N_G groups. The following assumptions must also hold:

- The cosmic signals are stationary for $N_t T_s$ seconds.
- The RFI signals are stationary for $N_{st} T_s$ seconds.
- The RFI signals are not stationary for $N_t T_s$ seconds.

The k^{th} short term covariance matrix estimate is given by

$$\widehat{\mathbf{R}}_k = \frac{1}{N_{st}} \sum_{n=(k-1)N_{st}+1}^{kN_{st}} \mathbf{y}(nT_s)\mathbf{y}(nT_s)^H \tag{9}$$

where $k \in \{1, \cdots, N_G\}$. The covariance matrix estimate can then be written as

$$\widehat{\mathbf{R}} = \frac{1}{N_G} \sum_{k=1}^{N_G} \widehat{\mathbf{R}}_k. \tag{10}$$

For each short term integration covariance matrix estimate $\widehat{\mathbf{R}}_k$, an orthogonal RFI projector $\mathbf{P}_k$, can be constructed, since the RFI is assumed stationary over the short term integration time ($N_{st} T_s$). The averaged orthogonal projected covariance matrix estimate is then

$$\begin{aligned}
\widehat{\mathbf{R}}_{orth} =& \frac{1}{N_G} \sum_{k=1}^{N_G} \mathbf{P}_k \widehat{\mathbf{R}}_k \mathbf{P}_k \\
=& \frac{1}{N_G} \sum_{k=1}^{N_G} \mathbf{P}_k (\widehat{\mathbf{R}}_c + \widehat{\mathbf{R}}_{k,r} + \widehat{\mathbf{R}}_n) \mathbf{P}_k \\
=& \frac{1}{N_G} \sum_{k=1}^{N_G} \mathbf{P}_k (\widehat{\mathbf{R}}_c + \widehat{\mathbf{R}}_n) \mathbf{P}_k \\
=& \frac{1}{N_G} \sum_{k=1}^{N_G} \mathbf{P}_k (\widehat{\mathbf{R}}_{cn}) \mathbf{P}_k.
\end{aligned} \tag{11}$$

Applying the matrix identity

$$\mathbf{vec}(\mathbf{ABC}) \equiv (\mathbf{C}^T \otimes \mathbf{A})\mathbf{vec}(\mathbf{B}), \tag{12}$$

where $\mathbf{vec}(\cdot)$ indicates the stacking of column vectors of a matrix and $\otimes$ the Kronecker product, to equation 11 yields

$$\begin{aligned}
\mathbf{vec}(\widehat{\mathbf{R}}_{orth}) &= \frac{1}{N_G} \sum_{k=1}^{N_G} (\mathbf{P}_k^T \otimes \mathbf{P}_k) \mathbf{vec}(\widehat{\mathbf{R}}_{cn}) \\
&= \left\{ \frac{1}{N_G} \sum_{k=1}^{N_G} (\mathbf{P}_k^T \otimes \mathbf{P}_k) \right\} \mathbf{vec}(\widehat{\mathbf{R}}_{cn}) \\
&= \mathbf{C}\mathbf{vec}(\widehat{\mathbf{R}}_{cn}).
\end{aligned} \tag{13}$$

The RFI is however assumed to be non-stationary over the total integration time $N_t T_s$, therefore, $\mathbf{P}_k$ will vary between the short term integration groups. The matrix $\mathbf{C}$ becomes non-singular if N_G is large enough and the orthogonal projectors vary sufficiently. The corrected covariance matrix is then

$$\widehat{\mathbf{R}}_{cn} = \mathbf{unvec}(\mathbf{C}^{-1}\mathbf{vec}(\widehat{\mathbf{R}}_{orth})), \tag{14}$$

where the $\mathbf{unvec}(\cdot)$ operator is the inverse of the $\mathbf{vec}(\cdot)$ operator in equation 12.

4.3. Oblique Projection

The oblique projection method projects along the RFI vector space V_r onto the cosmic vector space V_c. To construct this oblique projector it is required that the column vectors in $[\mathbf{A}_c \mathbf{A}_r]$ are independent ($V_r \cap V_c = \{\mathbf{0}\}$). The oblique projector is given by [1, p. 51]

$$\boldsymbol{E}_{V_r \to V_c} = \mathbf{A}_c (\mathbf{A}_c^H \mathbf{P}_{V_r}^{\perp} \mathbf{A}_c)^{-1} \mathbf{A}_c^H \mathbf{P}_{V_r}^{\perp}, \tag{15}$$

where $\mathbf{P}_{V_r}^{\perp}$ is an orthogonal projector which projects along V_r onto a vector space that is orthogonal to V_r. When an oblique projector is applied, the RFI is nulled and the cosmic signal is recovered, however the noise is biased

$$\begin{aligned}
\mathbf{R}_{obl} &= \boldsymbol{E}_{V_r \to V_c} \mathbf{R} \boldsymbol{E}_{V_r \to V_c}^H \\
&= \mathbf{R}_c + \boldsymbol{E}_{V_r \to V_c} \mathbf{R}_n \boldsymbol{E}_{V_r \to V_c}^H.
\end{aligned} \tag{16}$$

For the case when V_r and V_c are orthogonal, the oblique and orthogonal projectors are equivalent. The basis for V_c can be constructed from either a skymap or choosing an area of interest that does not contain the RFI.

4.4. Subspace Subtraction

If the power and the geometric delay vectors of the RFI sources are known, then the effect of the RFI sources can be subtracted [5, p. 115]

$$\mathbf{R}_{cn} = \mathbf{R} - \sum_{i=1}^{N_r} \sigma_i^2 \mathbf{a}_i \mathbf{a}_i^H. \tag{17}$$

The power of the RFI source and a basis for the geometric delay vectors can be estimated by using factor analysis, see section 4.5.

4.5. RFI Subspace Estimation

Any basis of the RFI subspace V_r can be used to construct the aforementioned projectors, not just $\mathbf{A}_r$. The ability of the projection and subtraction methods to null the contribution of RFI is dependent on the accuracy of the estimate of a basis set that spans the vector space V_r. When the direction of arrival of the RFI is not known, $\mathbf{A}_r$ cannot be calculated. However, an orthogonal set of eigenvectors can be found by applying eigenvalue decomposition (EVD) to the covariance matrix, because the covariance matrix is positive semi-definite [8, p. 517]. If it can be assumed that the cosmic signal contribution can be ignored, that the noise is independently and identically distributed and that the RFI signals are uncorrelated, then the EVD of the covariance matrix yields [1, p. 64-65]

$$
\begin{aligned}
\mathbf{R} \approx & \mathbf{R}_r + \mathbf{D}_n \\
= & \begin{bmatrix} \mathbf{M}_r & \mathbf{K}_r \end{bmatrix} \begin{bmatrix} \mathbf{D}_r & \mathbf{0} \\ \mathbf{0} & \mathbf{0} \end{bmatrix} \begin{bmatrix} \mathbf{M}_r^H \\ \mathbf{K}_r^H \end{bmatrix} + \sigma_n^2 \mathbf{I} \\
= & \begin{bmatrix} \mathbf{M}_r & \mathbf{K}_r \end{bmatrix} \mathbf{D}_{rn} \begin{bmatrix} \mathbf{M}_r^H \\ \mathbf{K}_r^H \end{bmatrix} \\
= & \begin{bmatrix} \mathbf{M}_r & \mathbf{K}_r \end{bmatrix} \begin{bmatrix} \mathbf{D}_r + \sigma_n^2 \mathbf{I}_{N_r} & \mathbf{0} \\ \mathbf{0} & \sigma_n^2 \mathbf{I}_{N_e - N_r} \end{bmatrix} \begin{bmatrix} \mathbf{M}_r^H \\ \mathbf{K}_r^H \end{bmatrix}, \quad (18)
\end{aligned}
$$

where

$\mathbf{M}_r$	is the eigenvectors that form the range of V_r,
$\mathbf{K}_r$	is the eigenvectors that form the kernel of V_r,
$\mathbf{D}_r$	is the matrix of eigenvalues ($\lambda_{r,j}$) for $\mathbf{R}_r$,
$\mathbf{D}_{rn}$	is the matrix of eigenvalues (λ_j) for $\mathbf{R}$.

The column vectors of $\mathbf{M}_r$ are orthogonal as well as those of $\mathbf{K}_r$. For the case where there are two or more RFI signals it is unlikely that $\mathbf{M}_r$ will be equal to $\mathbf{A}_r$. Therefore, the vector space V_r is spanned differently and the eigenvalues $\lambda_{r,j}$ will not be equal to the RFI powers $\sigma_{r,j}^2$ (however the total power will be the same). The noise only affects the eigenvalues of $\mathbf{R}_r$ but not its eigenvectors, because the noise is identically distributed [1, p. 65].

The orthogonal projector in equation 7 can now be constructed using $\mathbf{M}_r$, which is identified by the larger eigenvalues in $\mathbf{D}_{rn}$. One simple method [9] to identify the RFI is to count the eigenvalues which exceed three median absolute deviations from the median

$$
\lambda_j > 3 \cdot \text{median}(|\mathbf{D}_{rn} - \text{median}(\mathbf{D}_{rn})|) + \text{median}(\mathbf{D}_{rn}), \quad (19)
$$

where λ_j is the j^{th} eigenvalue contained in $\mathbf{D}_{rn}$. Using the median lessens the influence of outliers, that is, the values affected by the RFI. Alternative methods are given in [10, 11, 12].

If the noise is not identically distributed, then adding the noise covariance matrix $\mathbf{R}_n = \mathbf{diag}(\sigma_{n,1}^2, \ldots, \sigma_{n,n_e}^2)$ to the RFI covariance matrix $\mathbf{R}_r$ causes the eigenvectors[1] of the sum to change [1, p. 64-65].

When the instrumental noise is not calibrated for an interferometer, factor analysis [13] can be used. Factor analysis is a statistical method that decomposes a $p \times p$ covariance matrix, that is, $\mathbf{R} = \mathbf{Z}\mathbf{Z}^H + \mathbf{D}$, where $\mathbf{Z}$ is a $p \times q$ matrix and $\mathbf{D}$ is a $p \times p$ diagonal matrix. Applying this decomposition to an interferometer's covariance (the influence of the cosmic source is considered negligible) yields

$$
\begin{aligned}
\mathbf{R} = & \mathbf{Z}\mathbf{Z}^H + \mathbf{D} \\
= & \mathbf{R}_r + \mathbf{R}_n. \quad (20)
\end{aligned}
$$

This method places a restriction on the number of factors (that is interferers), namely $q < (p - \sqrt{p})$ [4, 13].

[1] However, if the power of the RFI is much larger than the noise power ($\sigma_{r,i}^2 \gg \sigma_{n,i}^2$), the effect of noise on the RFI covariance matrix's eigenvalues will diminish.

5. EXPERIMENTAL RESULTS

To show the effect of the spatial RFI mitigation methods, full sky dirty images were created by classical delay beamforming [1, p. 36] on each pixel. In figure 1 the RFI source is clearly seen at the top and its intensity is chosen as the 0 dB point. Data was also saved when the hexacopter was switched off and a ground truth image was created, see figure 2. In the ground truth image Cassiopeia A (the brightest source) and Cygnus A are clearly seen. When the orthogonal projector is applied it is seen in figure 3 that the strong cosmic sources are recovered, however, there is a null in the position where the RFI source was. Orthogonal projection with subspace bias correction recovers the information that was lost due to the orthogonal projection, as seen in figure 4. For the oblique projector a skymap was chosen that consists of Cassiopeia A and Cygnus A, see figure 5. The oblique projector recovers what was specified in the skymap and nulls everything else. Subspace subtraction seems to perform similarly to orthogonal projection with bias correction, however the reliability of the information recovered in the position of the RFI can be questioned, since this method effectively replaces the null with noise, see figure 6.

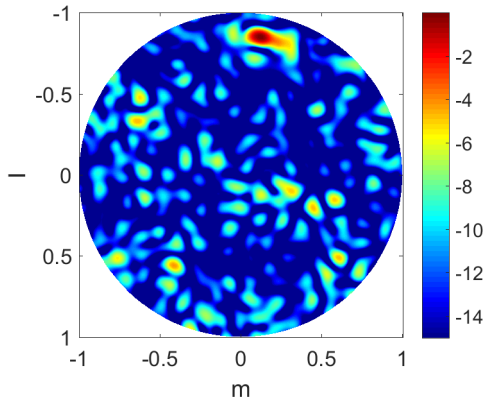

Fig. 1: Full skymap with RFI source visible at the top right in dB. All other sources are drowned in the sidelobe response of the RFI source. The power of the cosmic sources are at least 39 dB below that of the RFI source. The scale is set to saturate at -15 dB so that the RFI source is clearly visible.

As a figure of merit the Mean Absolute Percentage Error was chosen

$$
\mathbf{MAPE} = 100 \sum_i^{N_e} \sum_j^{N_e} \frac{|\widehat{\mathbf{R}}_{proj,i,j} - \widehat{\mathbf{R}}_{clean,i,j}|}{|\widehat{\mathbf{R}}_{clean,i,j}|} \quad (21)
$$

where $\widehat{\mathbf{R}}_{proj,i,j}$ is the ij^{th} element of the covariance matrices recovered with a spatial filtering method and $\widehat{\mathbf{R}}_{clean}$ is the ij^{th} element of the covariance matrix estimated from the data where the hexacopter is switched off. The results are given in

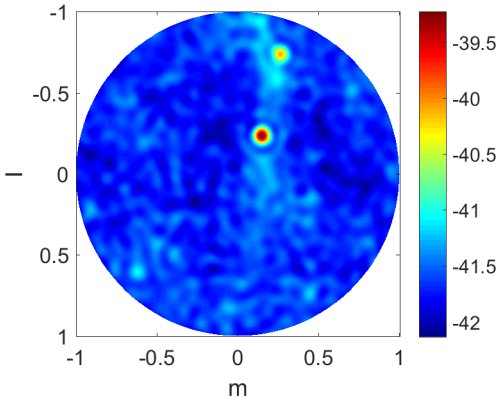

Fig. 2: Full skymap without RFI source in dB.

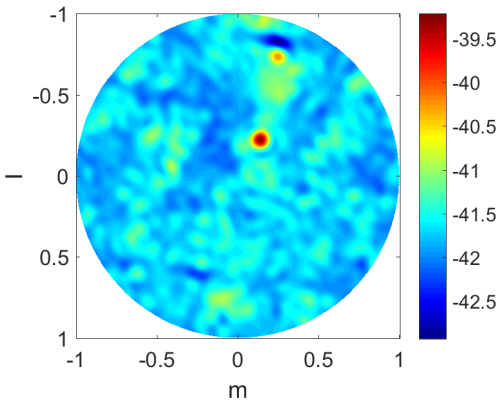

Fig. 3: Full skymap with RFI source removed using orthogonal projection in dB.

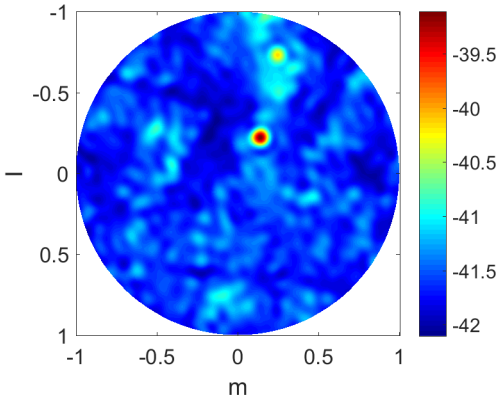

Fig. 4: Full skymap with RFI source removed using orthogonal projection with bias correction in dB.

a bar graph in figure 7. To make the comparison more meaningful the MAPE is also calculated between two different time step covariance matrices for when the hexacopter is switched

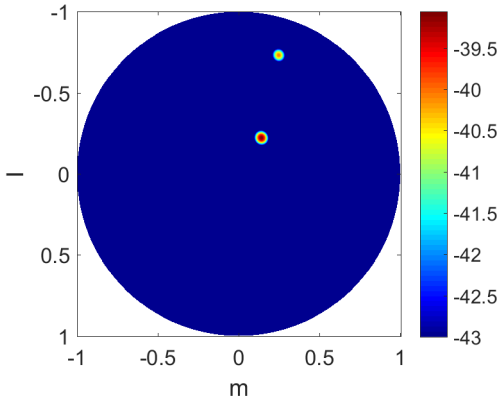

Fig. 5: Full skymap with RFI source removed using Oblique Projection in dB. The scale is set to saturate at -43 dB so that the recovered sources are clearly visible.

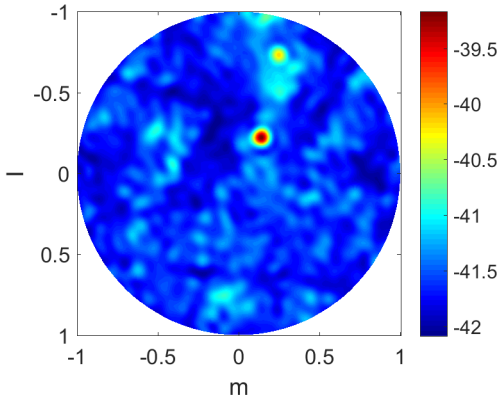

Fig. 6: Full skymap with RFI source removed using subspace subtraction.

off (this is labelled as clean). Any mitigation method that has a MAPE close to the clean MAPE is considered to have recovered the ground truth successfully. The orthogonal projector with subspace bias correction performs the best, however it is computationally the most expensive. The subspace subtraction method also performs well in recovering the ground truth. The oblique projector performs the poorest, since it was implemented only to recover the two bright cosmic sources.

To measure the ability of the mitigation methods to recover a source's power, the power of Cassiopia A in the RFI mitigated images is compared to that of the RFI free sky image, see figure 8. The percentage error in power is also calculated between two different time step images for when the hexacopter is switched off (this is labelled as clean). The oblique projector and orthogonal projection with subspace bias correction methods performs the best. However, all of the methods produced results with recovered power within 3.5% of the estimate of the source's power.

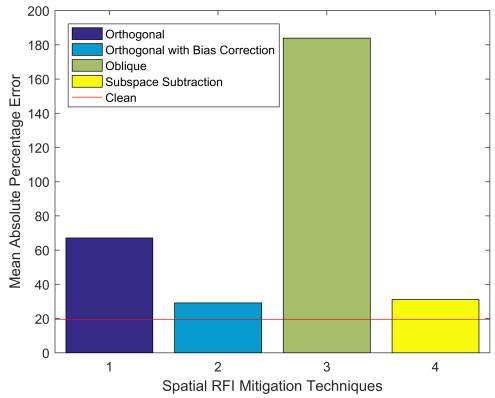

Fig. 7: MAPE of Spatial RFI Mitigation Techniques Covariance Matrices relative to RFI Free Covariance Matrix.

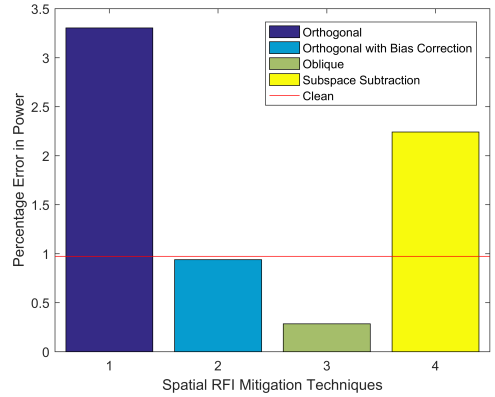

Fig. 8: Percentage error of power for Cassiopeia A.

6. CONCLUSION

The hexacopter signal was 40 dB above the cosmic signals and saturated the entire skymap. All of the projection methods that were implemented are able to remove the hexacopter signal and approximately recover the ground truth. If it is assumed that factor analysis is used to determine the RFI subspace then subspace subtraction has the lowest computational cost (since no projector needs to be constructed) followed by orthogonal projection. The oblique projector which includes first calculating the orthogonal projector and then the oblique projector has an increased computational cost. The orthogonal projector with subspace bias correction has the highest computational cost because the correction matrix $\mathbf{C}$ must be calculated and inverted. Orthogonal projection with bias correction performs the best in recovering the entire image (this is especially useful when the RFI source is in the desired field of view). The oblique projector performs well when a region is to be recovered where the RFI source is not located.

7. REFERENCES

[1] G. Hellbourg, *Radio Frequency Interference Spatial Processing for Modern Radio Telescopes*, Ph.D. thesis, University of Orleans, 2014.

[2] J. Raza, A. Boonstra, and A. van der Veen, "Spatial filtering of RF interference in radio astronomy," *IEEE SIGNAL PROCESSING LETTERS*, vol. 9, no. 2, pp. 64–67, February 2002.

[3] S. van der Tol and A. van der Veen, "Performance analysis of spatial filtering of RF interference in radio astronomy," *IEEE TRANSACTIONS ON SIGNAL PROCESSING*, vol. 53, no. 3, pp. 896–910, February 2005.

[4] A. van der Veen, A. Leshem, and A. Boonstra, "Signal processing for radio astronomical arrays," *IEEE Sensor Array and Multichannel Signal Processing Workshop*, pp. 1–10, July 2004.

[5] A. J. Boonstra, *Radio Frequency Interference Mitigation in Radio Astronomy*, Ph.D. thesis, Delft University of Technology, 2005.

[6] M. Zatman, "How narrow is narrowband?," *IEEE Proceedings-Radar, Sonar and Navigation*, vol. 2, no. 145, pp. 85–91, 1998.

[7] S. Kay, *Fundamentals of Statistical Signal Processing, Volume I: Estimation Theory*, Prentice-Hall, 1993.

[8] C. D. Meyer, *Matrix Analysis and Applied Linear Algebra*, SIAM: Society for Industrial and Applied Mathematics, 2001.

[9] J. Wagner, "C++ beamformer library with rfi mitigation," Tech. Rep., Max Planck Institute for Radio Astronomy, 2011.

[10] H. Akaike, "Information theory and an extension of the maximum likelihood principle," *Proc. 2nd Int. Symp. Inf. Theory*, pp. 267–281, 1973.

[11] M. Wax and I. Ziskind, "Detection of the number of coherent signals by the mdl principle," *IEEE Trans. Acoust., Speech, Signal Process.*, vol. 37, no. 7, pp. 1190–1196, Aug. 1989.

[12] M. S. Bartlett, "Tests of significance in factor analysis," *British J. Psych.*, vol. 3, pp. 77–85, 1950.

[13] A. M. Sardarabadi, *Covariance Matching Techniques for Radio Astronomy Calibration and Imaging*, Ph.D. thesis, Delft University of Technology, 2016.